A network diagram consisting of various sized light blue circles connected by thin white lines, set against a solid blue background. The circles are of different diameters and are scattered across the page, with some larger circles acting as central nodes.

Joint Research Programme  
BTO 2021.027 | April 2021

**Impact of ionic  
composition of  
groundwater on  
oxidative iron  
precipitation**

Joint Research Programme

**KWR**

Bridging Science to Practice



# Report

## Impact of ionic composition of groundwater on oxidative iron precipitation

**BTO 2021.027 | April 2021**

This research is part of the Joint Research Programme of KWR, the water utilities and Vewin.

### Project number

402045-031

### Project manager

Erwin Beerendonk

### Client

BTO - Thematic research - Purification

### Author(s)

dr.ir. D. Vries, dr.ir. M. Korevaar, ir. L. de Waal, dr. ir. A. Ahmad

### Quality Assurance

Dr. ir. E. Cornelissen

### Sent to

This report is distributed to BTO-participants and is public.

### Keywords

precipitation, groundwater treatment, iron

Year of publishing  
2021

### More information

dr.ir. D. Vries  
T +31 (0)30 6069 671  
E [dirk.vries@kwrwater.nl](mailto:dirk.vries@kwrwater.nl)

PO Box 1072  
3430 BB Nieuwegein  
The Netherlands

T +31 (0)30 60 69 511  
F +31 (0)30 60 61 165  
E [info@kwrwater.nl](mailto:info@kwrwater.nl)  
I [www.kwrwater.nl](http://www.kwrwater.nl)

The logo for KWR (Knowledge and Water Research Institute) consists of the letters 'KWR' in a bold, blue, sans-serif font.

April 2021 ©

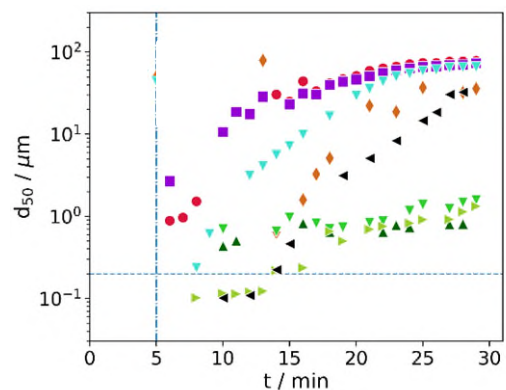
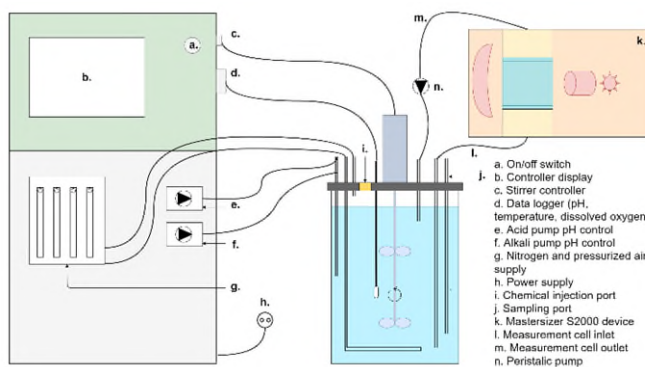
All rights reserved by KWR. No part of this publication may be reproduced, stored in an automatic database, or transmitted in any form or by any means, be it electronic, mechanical, by photocopying, recording, or otherwise, without the prior written permission of KWR.

# BTO Managementsamenvatting

## Ion-samenstelling is van grote invloed op doeltreffendheid grondwaterbehandeling

**Auteurs** dr.ir. Dirk Vries, dr.ir. Martin Korevaar

Dit onderzoek biedt inzicht in de interactie tussen verschillende ionen de groei van ijzer-neerslagen beïnvloeden. Dit helpt bij het vinden van effectievere operationele maatregelen voor ontijzering om m.n. vorming van colloïdaal ijzer(Fe) tegen te gaan, bijvoorbeeld door het plaatsen van ontharders *na* snelle zandfilters (RSF). Onttrokken grondwater is over het algemeen anaeroob en vereist dus beluchting, gevolgd door zandfiltratie om metalen zoals ijzer, maar ook ammonium te verwijderen. Neerslag van Fe zonder verdergaande coagulatie kunnen verantwoordelijk zijn voor een verminderde verwijdering van ijzer en andere metalen en doorbraak van colloïdale ijzerdeeltjes. Tests zijn uitgevoerd waarin de ijzeroxidatie en -precipitatie in de bovenwaterlaag van een RSF is nagebootst, waar de precipitatie voornamelijk plaatsvindt. Gebruik is gemaakt van een beluchte, continu geroerde tank op laboratoriumschaal. De resultaten tonen aan dat (a)  $\text{HCO}_3^-$  geen significante invloed heeft op de neerslag van Fe, (b) toevoeging van silicaat in aanwezigheid van  $\text{HCO}_3^-$  resulteert in verminderde Fe-neerslag, (c) NOM, in aanwezigheid van  $\text{HCO}_3^-$ , de neerslag van Fe drastisch belemmert en (d) toevoeging van Ca de Fe-neerslag verbetert in aanwezigheid van Si, NOM en  $\text{HCO}_3^-$ .



Links: experimentele proefopstelling in het laboratorium met de pH- en doseerregelaar aan de linkerkant van het vat, het lichtverstrooiingsapparaat (oranje) aan de rechterkant en het vat zelf dat is uitgerust met sensoren en slangen. Rechts: de  $d_{50}$  voor verschillende oplossingen (zie figuur 4B voor de legenda).

### Belang: beter inzicht in grondwaterzuivering leidt tot kennisgedreven optimalisatie van de bedrijfsvoering

Voor het verwijderen van metalen zoals ijzer (Fe) en ammonium wordt bij de behandeling van grondwater op drinkwaterproductielocaties veelvuldig snelle zandfiltratie (RSF) toegepast, gecombineerd met beluchting en eventuele ontgassing. Hierbij oxideert het ijzer en slaat vervolgens neer om te coaguleren tot grotere, filtreerbare deeltjes. Oxidatie kan worden vertraagd in aanwezigheid van P, Si of humuszuren. Bovendien

zijn ionsterkte en oxyanionen ook van invloed op de lading van de Fe(III)oxide-neerslag, en kunnen deze de effectiviteit van neerslag en daaropvolgende samenklontering beïnvloeden, wat leidt tot verschillende mate van filtreerbaarheid. Wanneer deeltjes niet voldoende groot (filtreerbaar) worden leidt dit tot een beperkte verwijdering van metalen als Fe, en het doorslaan van deze colloïdale ijzerdeeltjes. Het is echter nog niet duidelijk hoe de watersamenstelling (ionen en pH) deze groei van ijzerdeeltjes beïnvloedt. Bovendien kan de

samenstelling van het grondwater als gevolg van de verwerking van mineralen veranderen, mede onder invloed van klimaatverandering. Daarom moeten sommige grondwaterbehandelingslocaties wellicht worden geëvalueerd en nader onderzocht om na te gaan of aanvullende maatregelen nodig zijn om het Fe- en andere metaalgehalte in drinkwater op een aanvaardbaar niveau te houden. Om de drinkwaterproductie en het beheer van waterbronnen onder veranderende omstandigheden te optimaliseren, is het de moeite waard de mechanismen te onderzoeken die ten grondslag liggen aan de wisselwerking tussen neerslag, colloïdale stabiliteit en oxidatie, en tegelijkertijd experimentele en operationele gegevens te verzamelen om de modellering van deze verschijnselen te onderbouwen.

#### **Aanpak: analyse van lichtverstrooiing en chemische samenstelling**

Er werd gebruik gemaakt van een opstelling met een geroerd vat, gekoppeld aan een lichtverstrooiingsapparaat. Verschillende watersamenstellingen met variaties in alkaliniteit, calcium, silica, fosfaat en opgelost natuurlijk organisch materiaal werden gesynthetiseerd om het ontstaan van neerslag en huncoagulatie te onderzoeken. Lichtverstrooiingsmetingen en monsters werden gedurende 30 minuten genomen in een continu geroerd, belucht vat. De watermonsters werden geanalyseerd op metalen, bicarbonaat en calcium. Uit de lichtverstrooiingsmetingen werd de deeltjesgrootte van de gevormde vlokken bepaald.

#### **Resultaten: geen effect van alkaliniteit, calcium verbetert de neerslag bij aanwezigheid van NOM**

Verschillende  $\text{HCO}_3^-$ -concentraties hebben geen significante invloed op de coagulatiesnelheid van Fe en Fe wordt binnen de typische verblijftijd van grondwaterzuiveringsinstallaties volledig verwijderd. Silicaat toevoegingen in aanwezigheid van  $\text{HCO}_3^-$  resulteren in verminderde Fe-neerslag en zeer beperkte samenklontering, waarschijnlijk vanwege ladingsrepulsie door de negatief geladen Fe(III)oxide-neerslagoppervlakte. De toevoeging van NOM, belemmert de neerslag van Fe drastisch, mogelijk door de vorming van oplosbare Fe(III)-NOM

complexen. Toevoeging van Ca verbetert de neerslag van Fe in aanwezigheid van Si en NOM, wat kan worden toegeschreven aan een ladingneutraliserend effect van Ca. Toevoeging van fosfaat vermindert de groei van deeltjes, maar er is meer onderzoek nodig om dit te begrijpen.

#### **Toepassing: verwijdering van ijzer wordt beïnvloed door de samenstelling van grondwater**

De samenstelling van het grondwater heeft een grote invloed op het verwijderingsrendement van ijzer. Operationele maatregelen gericht op destabilisering van de colloïdale ter bevordering van de coagulatie, kunnen het verwijderingsrendement van RSF verbeteren. Wanneer het grondwater rijk is aan opgeloste organische stoffen of silicaat kan de efficiëntie worden verhoogd door kalkrijkwater bij te mengen of ontharders *na* de snelle zandfilterstap te plaatsen. Ook zou de organische stof kunnen worden verwijderd door een ionenwisselaar voor de snelle zandfilterstap te plaatsen.

#### **Het Rapport**

Dit onderzoek is beschreven in het rapport *Invloed van de ion-samenstelling van het grondwater op de oxidatieve neerslag van ijzer* (BTO-2021.027) en is ingediend voor publicatie in *Water Science and Technology*.

## Bedrijfsparagraaf

Snelle zandfilters zijn de geijkte techniek om ijzer- en mangaan te verwijderen. Ondanks de opkomst van nieuwe technieken zal dit ook in de toekomst zo blijven. Daarom is het van belang dat waterbedrijven grip hebben op de mechanismes die relevant zijn voor ijzer- en mangaanverwijdering door snelle zandfilters. Helaas is dit lang niet altijd het geval waardoor de filters meer op basis van ervaring dan op basis van wetenschap worden bestuurd.

Zo is de invloed van de watersamenstelling op de ijzerverwijdering nog niet volledig begrepen. In dit onderzoek is dit daarom systematisch onderzocht in de context van een bovenwaterlaag, die is gesimuleerd met een continu geroerd vat. Er is met name gekeken naar de groei en filtereerbaarheid van ijzerprecipitaten als functie van tijd. Om aan te sluiten bij de praktijk van snelle zandfilters is gekeken naar de precipitaatgroei in de eerste 30 minuten na het begin van oxidatie, dat wil zeggen een duur waarbinnen de typische verblijftijd in snelle zandfilters valt.

Uit de experimenten blijkt dat de invloed van de waterkwaliteit groot is; de verschillende concentraties van de onderzochte stoffen zijn gekozen in lijn met typische concentraties in grondwaterwinningen in Nederland. In de afwezigheid van calcium, zijn de ijzerprecipitaten colloïdaal stabiel wanneer er silica, fosfor of DOC aanwezig is; deze ijzerprecipitaten blijven dus klein en zijn niet filterbaar. De invloed van  $\text{HCO}_3^-$  is aanwezig maar klein. De toevoeging van calcium destabiliseert de colloïden wat betekent dat ze sneller groeien en dus beter filterbaar zijn. Dit effect is vooral sterk bij DOC.

In de praktijk zal er altijd wel calcium aanwezig zijn in het behandelde grondwater, waardoor de kans op

een volledige falende ontijzering doordat ijzer colloïden te stabiel zijn niet groot is. Maar tegelijkertijd is er ook altijd DOC aanwezig in de bronnen, wat voor een suboptimale ijzerverwijdering door stabiele ijzercolloïden kan zorgen. De vraag die in de praktijk dus gesteld moet worden is of er in het ruwe water genoeg calcium zit om de negatieve invloed van het aanwezige DOC op de ijzerverwijdering te compenseren. Hetzelfde verhaal geldt voor mindere mate ook voor de negatieve invloed van silica en fosfor. Dit pleit er dan ook voor dat in sommige gevallen de ontharding pas na het zandfilter te laten plaatsvinden, zodat het calcium van het ruwe water zijn positieve effect op de ijzerverwijdering kan laten gelden.

De mate van stabiliteit van de colloïden bepaalt hoe snel de ijzerprecipitaten groeien. Zeer stabiele colloïden zullen niet uitgroeien tot een filterbare grootte en daardoor niet verwijderd worden. Maar te snel groeiende precipitaten (doordat ze colloïdaal instabiel zijn) kunnen ervoor zorgen dat ze alleen worden afgevangen in het bovenste gedeelte van het bed. Dit betekent dus dat niet de capaciteit van het hele bed wordt gebruikt waardoor de drukvalk snel stijgt en er sneller moet worden teruggespoeld. Inzichten uit dit onderzoek bieden dus ook hier aanknopingspunten om de bedrijfsvoering aan te passen om de terugspoelfrequentie te optimaliseren.

De resultaten geven een kwalitatieve beschrijving van de invloed van verschillende waterkwaliteitsparameters. Om tot een modelgestuurde operatie van de zuivering te komen zullen deze effecten nauwkeuriger moeten worden gekwantificeerd waarvoor meer onderzoek nodig is. De visie waarbinnen dit onderzoek moet plaatsvinden wordt opgesteld in het BTO onderzoek "Kennis boven water" en uitgewerkt op basis van een praktijkinventarisatie en uitgebreide literatuurstudie.

# Contents

<i>BTO Managementsamenvatting</i>	<b>3</b>
<i>Bedrijfsparagraaf</i>	<b>5</b>
Contents	<b>6</b>
Abstract	<b>7</b>
<b>1 Introduction</b>	<b>8</b>
<b>2 Materials and Methods</b>	<b>9</b>
2.1 Initial solutions	9
2.2 Iron oxidation and precipitation experiments	11
2.3 Particle characterization	12
<b>3 Results and discussion</b>	<b>13</b>
3.1 Impact of bicarbonate	13
3.2 Impact of oxyanions and natural organic matter	13
3.3 Impact of calcium	15
<b>4 Conclusions and implications</b>	<b>17</b>
Acknowledgements	19
<b>I References</b>	<b>20</b>
<b>II Supplementary material</b>	<b>22</b>
References	26

## Abstract

In the Netherlands, approximately 60% of drinking water is obtained from groundwater. Raw groundwater generally is anaerobic and thus requires aeration followed by rapid sand filtration (RSF) to remove iron, manganese, arsenic and ammonium. The mechanisms responsible for the removal of different constituents, clogging of RSFs and breakthrough of colloidal iron or manganese oxides have not been fully elucidated in previous studies. In this work, factors affecting iron precipitation and co-precipitation of other ions have been studied in a laboratory simulated environment of the supernatant layer of submerged sand filters is studied through the use of an aerated, continuously stirred bench scale jar experiments. Time series data of the iron concentration of filtered samples and precipitate size have been collected in experiments with synthetic groundwater solutions with varying concentrations of P, Si,  $\text{HCO}_3^-$  and Ca at neutral pH. We show that different  $\text{HCO}_3^-$  concentrations have no significant impact on the precipitate growth kinetics of Fe, silicate additions in the presence of  $\text{HCO}_3^-$  result in reduced Fe precipitate growth, and NOM, in the presence of  $\text{HCO}_3^-$ , drastically hampers the precipitation rate of Fe. The addition of P appears to hamper precipitate growth to some extent, but more research is needed to understand the impact of P on Fe precipitation. We also observe that addition of Ca improves the growth of Fe precipitates in the presence of Si and NOM. These results have great significance for improving Fe removal efficiency of groundwater treatment plants in Netherlands and abroad.

*Keywords: groundwater treatment, iron oxidation, precipitation, rapid sand filtration*



# 1 Introduction

In the Netherlands, 60% of drinking water is obtained by treating groundwater, mostly by aeration and rapid sand filtration to remove impurities such as iron (Fe), manganese (Mn), arsenic (As) and ammonium ( $\text{NH}_4^+$ ). Drinking water in the Netherlands is generally of high quality, however in some cases discolouration events due to incomplete removal of Fe from groundwater are reported. Therefore, this study is focused on improving the efficiency of groundwater treatment for effective Fe removal.

When anaerobic groundwater is aerated at water treatment plants e.g. by cascades, oxygen ( $\text{O}_2$ ) diffuses into groundwater and facilitates oxidation of dissolved Fe(II) to insoluble Fe(III)(oxyhydr)oxide precipitates. The Fe(III)(oxyhydr)oxide precipitates are typically removed in submerged rapid sand filters (van Beek et al., 2016; Vries et al., 2017). The ionic composition of groundwater has a major impact on the structure, crystallinity and aggregation behaviour of these Fe(III) precipitates. Previous studies have shown that at near-neutral pH, Fe(II) oxidation by  $\text{O}_2$  leads to the formation of moderately crystalline Fe(III) precipitates, such as lepidocrocite, whereby the presence of oxyanions such as silicate (Si), phosphate (P) and arsenate ( $\text{As(V)}$ ) in water leads to the formation of poorly ordered Fe(III) phases (Senn et al., 2015; van Genuchten et al., 2014; Voegelin et al., 2010). The presence of oxyanions during Fe(III) precipitation not only affect the local coordination and ordering in the Fe(III) precipitates, but also decrease the extent of particle aggregation due to a highly negative surface charge which causes repulsion between the particles. This may result in stable colloidal suspensions, especially in solutions devoid of Ca and Mg cations, which are difficult to clarify by sedimentation and/or filtration. Bivalent cations such as Ca and Mg can counteract this repulsion effect of negative particle surface charge and can enhance particle aggregation (Ahmad et al., 2020; Ahmad et al., 2019a; Ahmad et al., 2019b; Senn et al., 2015). Calcium is also known as a dominant coagulating agent for solutions containing NOM and other ions (Sholkovitz and Copland, 1981) and is expected to compete with trace metals for binding with NOM (Tipping, 1993; van den Hoop et al., 1995).

In the Netherlands, the ionic composition of groundwater significantly varies from one groundwater source to another. The impact of variations in key groundwater solutes, including bicarbonate ( $\text{HCO}_3^-$ ), Si, P, NOM and Ca on Fe(III) precipitation and removal at groundwater treatment plants is not yet fully understood. Most groundwater treatment systems are still designed on rules of thumb without detailed understanding of physicochemical processes. Although the oxidation and precipitation and subsequent aggregation and coagulation of Fe (see e.g. (Bratby, 2016; Jarvis et al., 2006; Sholkovitz and Copland, 1981)) has been studied before, the rate of precipitation in relation to variations in the composition of groundwater has not received much attention. The residence time in groundwater treatment installations and the half-life of Fe(II) oxidation are comparable (Stumm and Morgan, 1996; Vries et al., 2017). Hence, we believe that the investigation of the kinetics of Fe(III) precipitation due to Fe(II) oxidation are critical for improving the efficiency of rapid sand filters. In this work, we study the rate of precipitation of Fe by oxidizing Fe(II) in simulated groundwater matrices whereby the ionic composition, i.e.  $\text{HCO}_3^-$ , NOM, Si, Ca and P concentration, is determined by the groundwater quality in the Netherlands. To investigate the precipitation kinetics in the supernatant layer of a submerged sand filter, we use a laboratory simulated environment through the use of an aerated, continuously stirred bench scale jar experiments. It is expected that, in line with what has been published (Jobin & Ghosh, 1972), alkalinity should not impact Fe(II) oxidation at neutral pH, while Ca should have a positive effect on the Fe precipitation rate while Si, P and NOM should have a negative effect (Tipping, 1993; van den Hoop et al., 1995).

## 2 Materials and Methods

### 2.1 Initial solutions

Iron oxidation and precipitation rate experiments were performed with different initial solutions (Table 1), produced by dosing chemical stocks in ultrapure water (Milli-Q, produced by purifying distilled water with a Purelab Chorus provided by Veolia). All the initial solutions contained 80.5  $\mu\text{M}$  Fe(II), 8.2  $\mu\text{M}$  Mn(II), 0.60  $\mu\text{M}$  As(III) and 460  $\mu\text{M}$  NaCl, but differed in the concentration of  $\text{HCO}_3^-$  (1500-300  $\mu\text{M}$ ), Si (320-640  $\mu\text{M}$ ), P (15  $\mu\text{M}$ ), DOC (150-300  $\mu\text{M}$ ) and Ca (450-1800  $\mu\text{M}$ ) (See Table 1). These differences in ionic composition were chosen to simulate groundwater quality in the Netherlands. For preparing the stock solutions, reagent grade chemicals were used. Stock solutions of 22.4 g/L  $\text{FeSO}_4$ , 61.9 g/L  $\text{NaHCO}_3$ , 13.5 g/L NaCl and 1.0 g/L  $\text{Na}_2\text{SiO}_3$  were prepared by dissolving  $\text{FeSO}_4 \cdot 7\text{H}_2\text{O}$  (CAS: 10025-77-1, 97% purity, J.T Baker The Netherlands),  $\text{NaHCO}_3$  (CAS: 144-55-8, >99% purity, J.T Baker The Netherlands), NaCl (CAS: 7647-14-5, 99% purity, J. T Baker The Netherlands) and  $\text{Na}_2\text{SiO}_3 \cdot 5\text{H}_2\text{O}$  (CAS: 10213-79-3, 99% purity, Sigma-Aldrich) respectively in ultrapure water. The stock solutions of 49.8 g/L  $\text{CaCl}_2$  and 1.0 g/L  $\text{NaH}_2\text{PO}_4$  were prepared by dissolving  $\text{CaCl}_2$  anhydrous (CAS: 10043-52-4, 96% purity, J. T Baker) and  $\text{NaH}_2\text{PO}_4 \cdot \text{H}_2\text{O}$  (CAS: 10049-21-5, >98% purity, J.T Baker) respectively in 0.1 M HCl. The NOM stock solution of 2.4 g/L DOC was prepared by diluting a primary stock (HumVi, Vitens, The Netherlands, 117.4 g/L DOC) that contained ca. 75% humic substances (HS) (Ahmad et al., 2020), see the composition in Table S1, supplementary material. Arsenic was dosed using a stock solution of 1.0 g/L  $\text{As}_2\text{O}_3$  (CAS: 1327-53-3, 99% purity, Inorganic Ventures). For pH adjustment, 0.1 M HCl or 0.1 M NaOH were used.

Table 1: Composition of the initial solutions used in the precipitation experiments. In all the initial solutions the concentration of Fe(II), Mn(II) and As(III) was 81, 8.2 and 0.6  $\mu\text{M}$ . All the initial solutions also contained 460  $\mu\text{M}$  NaCl.

Impact of ion(s)	Experimental code	Concentration ( $\mu\text{mol/L}$ )				
		HCO <sub>3</sub>	Si	P	DOC	Ca
HCO <sub>3</sub>	1500HCO3	1475				
	1800HCO3	1844				
	2200HCO3	2213				
	2600HCO3	2581				
	3000HCO3	2950				
Oxyanions	2200HCO3 + 320Si	2213	320			
	2200HCO3 + 640Si	2213	641			
	2200HCO3 + 15P	2213		15		
	2200HCO3 + 150DOC	2213			150	
HCO <sub>3</sub> + Ca	1500HCO3 + 900Ca	1475	0			898
	2200HCO3 + 900Ca	2213	0			898
	3000HCO3 + 900Ca	2950	0			898
HCO <sub>3</sub> + oxyanion + Ca	2200HCO3 + 320Si + 450 Ca	2213	320			449
	2200HCO3 + 320Si + 900Ca	2213	320			898
	2200HCO3 + 320Si + 1800Ca	2213	320			1796
	2200HCO3 + 150DOC + 900Ca	2213			150	898
	2200HCO3 + 300DOC + 900Ca	2213			300	898

## 2.2 Iron oxidation and precipitation experiments

Iron oxidation and precipitation rate experiments were performed with a 5 liter glass vessel connected to a controller (ez-Control, Applikon® Biotechnology) for adjusting, maintaining and logging (BioXpertV2 software) the pH, temperature, air supply and stirring speed (Fig. 1). The experiments were carried out at pH 7.0 and 20 °C, with stirring set to 300 rpm for the first 5 minutes and 80 rpm for the rest of the experiment. The experimental procedure included: (i) preparation of the initial solutions in the oxygen-depleted reaction vessel and collection of solution samples for control, (ii) O<sub>2</sub> dosing to allow precipitation of Fe(III) while the suspension was stirred and (iii) collection of suspension samples after 30 minutes, which were filtered over 0.20 µm filters (SpartanTM 30/0.20 RC 0.20 µm syringe filters (GE Healthcare, Buckinghamshire, UK)) to determine the removal of Fe(III) precipitates and co-precipitated species. The removal of Fe was determined from the difference between the measured values of the initial solution and final filtered solution.

Fe, Mn, As, Ca, Si, P were measured by Inductively Coupled Plasma Mass Spectrometry (ICP-MS) (XSERIES 2, Thermo Fisher Scientific, The Netherlands) using the collected samples before supplying air to the vessel (t=0 min.) and after 30 minutes. Samples for analysis by ICP-MS were preserved immediately after collection by dosing 50 µL 65% HNO<sub>3</sub> per 50 mL sample and stored at 4 °C. The analysis of DOC in water samples was carried out with a TOC-V<sub>CPH</sub> total organic carbon analyser (Shimadzu Benelux, 's-Hertogenbosch, The Netherlands). The samples for DOC analysis were conserved immediately after collection by adding 200 µL 30% HCl solution to 100 mL of sample which was closed off airtight and stored at 4 °C. Bicarbonate was analysed by a colorimetric method (HI-3811, Hanna Instruments) using HI 775-26 fresh water alkalinity reagent.

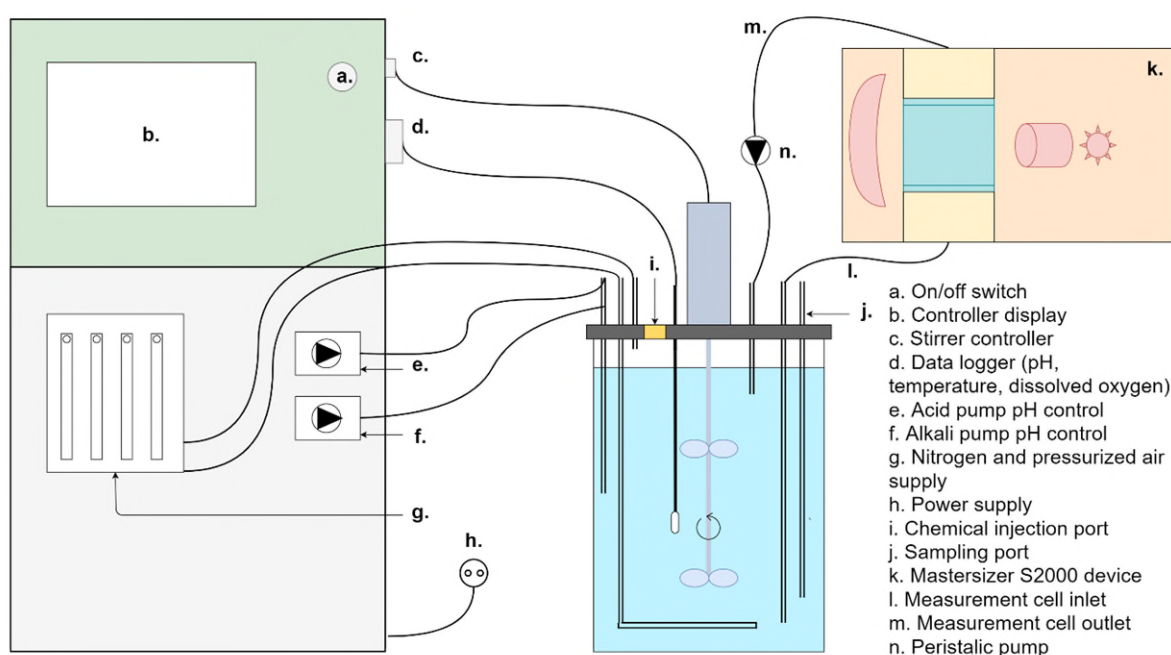


Figure 1: A schematic overview of the experimental set-up.

### 2.3 Particle characterization

The size and volume fraction of the precipitates was determined during the experiments by Multiple Light Scattering (MLS) using the Mastersizer 2000 (Malvern Instruments, UK). The MLS device was connected to the reaction vessel (Fig. 1) and the suspension was continuously drawn through the Mastersizer measurement cell at a constant flow of 216 mL/min using a masterflex easy-load II peristaltic pump combination (Metrohm Nederland B.V. The Netherlands). Malvern instruments Mastersizer 2000 software v5.61 recorded the particle size distribution every 20 s, for the complete duration of the experiment (30 min). A scattering coefficient<sup>1</sup> of 2.9 was used to determine the particle size of Fe(III)(oxyhydr)oxide particles (Gregory, 2009). From the light scattering data, relative precipitate volume and the size distribution have been determined. The relative precipitate volume is the ratio of the volume of the precipitate with respect to the total volume of the measurement cell. It is assumed that detected particles do not represent Fe(III)(oxyhydr)oxide particles if the diameter of 50% percent of the particles (i.e. d50) is larger than 300  $\mu\text{m}$ . This threshold is selected based on the observation that the diameter of 90% of the particles (i.e. d90) never exceeds 300  $\mu\text{m}$ . The relative precipitate volume and d50 are omitted from the results at the times this particle size threshold is exceeded.

---

<sup>1</sup> The scattering coefficient is a measure of the ability of particles to scatter photons out of a directed beam of light. This can be related to the particle's size

## 3 Results and discussion

### 3.1 Impact of bicarbonate

The percentage of residual Fe after filtration through a 0.20  $\mu\text{m}$  filter and relative precipitate volume as a function of different  $\text{HCO}_3^-$  concentrations are shown in Figure 2A and 2B respectively. Figure 2A shows that residual Fe quickly depletes by oxidation and reaches to complete absence for all the  $\text{HCO}_3^-$  concentrations in approximately 7 minutes. The relative precipitate volume appears to stabilize in approximately 15 minutes for all the  $\text{HCO}_3^-$  concentrations, except that of 1500  $\mu\text{M}$   $\text{HCO}_3^-$  which is the lowest  $\text{HCO}_3^-$  concentration. At this concentration the relative precipitate volume stabilizes already in 7 minutes. The particle size show the same trend as the relative precipitate volume, i.e. the  $d_{50}$  reaches approximately 100  $\mu\text{m}$  after 30 minutes (Figure S1-A, supplementary material). These results are in agreement with the findings of (Jobin and Ghosh, 1972) who showed that Fe(II) oxidation is only hampered when the buffer intensity is sufficiently large (i.e. in the order of  $4 \cdot 10^{-3} \text{ eq CaCO}_3/\text{pH}$ , hence an alkalinity of more than 16 mmol/L as  $\text{HCO}_3^-$  at neutral pH, which is substantially higher than the highest  $\text{HCO}_3^-$  concentration of 2600  $\mu\text{mol/L}$  used in this study. These results show that different  $\text{HCO}_3^-$  concentrations have no significant impact on the precipitation of Fe and precipitation is completed quite rapidly when the typical residence times of 15 to 30 minutes for groundwater treatment plants are considered.

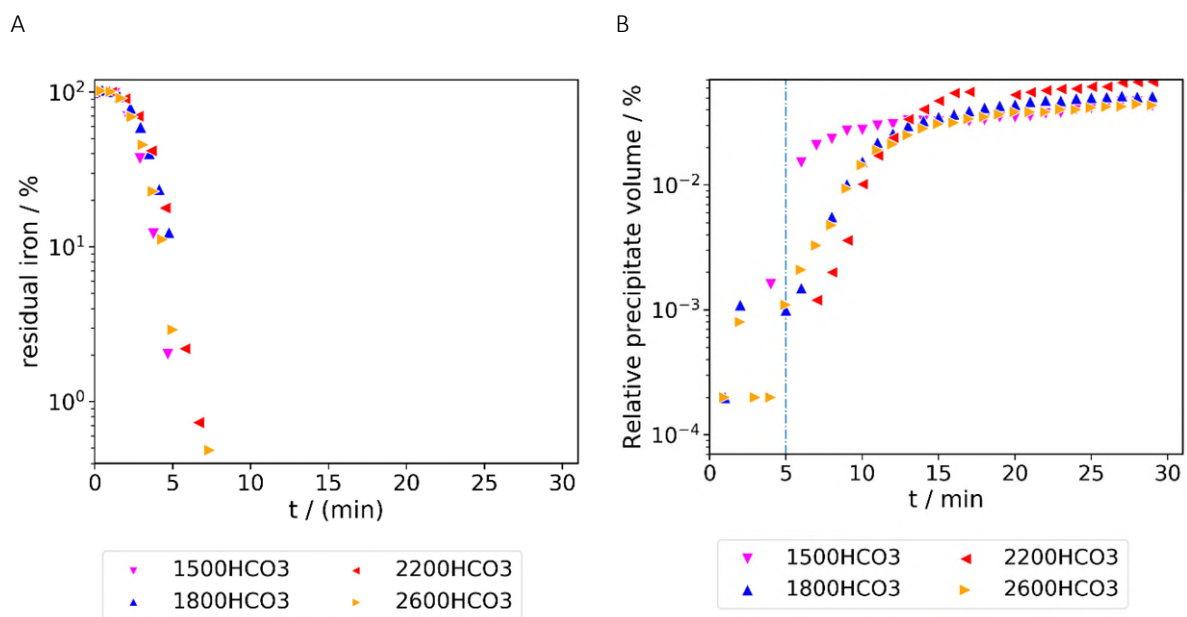


Figure 2: (A) Residual iron (%) after filtration through a 0.2 $\mu\text{m}$  filter and (B) precipitate volume relative to the total measured volume, as a function of different  $\text{HCO}_3^-$  concentrations.

### 3.2 Impact of oxyanions and natural organic matter

The % of residual Fe after filtration through 0.20  $\mu\text{m}$  filter and relative precipitate volume as a function of different Si, P and NOM concentrations in the presence of 2200  $\mu\text{M}$   $\text{HCO}_3^-$  are shown in Figure 3A and 3B respectively. Figure 3A shows that the % of residual Fe concentration stays approximately 100% for most samples, i.e. no significant Fe removal was observed except for the 30 min sample of 15  $\mu\text{M}$  P addition. In all

cases, the relative precipitation volume (Figure 3B) signal was also unstable, indicating a poor Fe precipitation. The poor Fe precipitation due to Si additions are in agreement with previous studies (Kinsela et al., 2016; Liu et al., 2007; Piispanen & Sallanko, 2011). Silicate ions bind strongly to Fe(III) precipitate surfaces during Fe(III) polymerization, which modifies two key properties of the suspension. First, by binding strongly to crystal growth sites on the Fe(III) precipitate surface, oxyanions inhibit the formation of crystalline Fe(III) minerals (i.e. lepidocrocite), leading to formation of poorly-ordered Fe(III) precipitates with a large specific surface area (van Genuchten et al., 2014b; Voegelin et al., 2010). Second, sorption of Si leads to negatively charged Fe(III) precipitate surfaces (Delaire et al., 2016; Kanematsu et al., 2013). Therefore, Si sorption generates particles with highly negative surface charge that are less likely to aggregate. The work of Piispanen et al. shows empirically that if the molar Si/Fe ratio exceeds 2.5, extremely small sized Fe particles are formed. In our study, the molar ratio of Si/Fe in the initial solution was in the range of 4-8, thus much higher. The particle size at t=30 minutes is 7 to 10  $\mu\text{m}$  after 30 minutes, hence an order of magnitude smaller than the case without Si (Figure S1-B, supplementary material).

These observations related to NOM additions are in agreement with several previous studies which also report a similar reduction in the removal of Fe(III) in the presence NOM (Ahmad et al., 2019a; Davis and Edwards, 2017; Gu et al., 1995; Ritter, 2005). The suppression of Fe(III) removal by filtration has been attributed to formation of soluble Fe(III)–NOM complexes, as well as formation of Fe(III)–NOM and Fe(III)(oxyhydr)oxide–NOM colloids. However, the identity of the particles (Fe(III)–NOM or Fe(III)(oxyhydr)oxide–NOM colloids) was not investigated in our study. Moreover, the properties of the soluble fraction of Fe(III)–NOM complexes remain unclear.

Regarding the behaviour of P in our study, sequential precipitation of different Fe(III) phases could be responsible for the initial stability and later destabilization of the suspension at 30 min to result in a lower residual Fe concentration after 0.20  $\mu\text{m}$  filtration. In previous studies of Fe(II) oxidation in the presence of P, precipitation of Lp-like material has been observed due to the sequential uptake of P during precipitate formation (Senn et al., 2015; Senn et al., 2018; van Genuchten et al., 2014a; Van Genuchten et al., 2014b; Voegelin et al., 2010; Voegelin et al., 2013). With the initial P/Fe(II) molar ratio of 0.55 (critical ratio) or higher, only P gets removed from solution and Fe(II) oxidation leads to exclusive formation of amorphous Fe(III)-phosphate. However, at initial P/Fe < critical P/Fe such as in our study where P/Fe is 0.2, multiple phases can be formed, including first the precipitation of polymeric Fe(III) phosphate and after depletion of P from solution, formation of more crystalline iron oxide phases takes place (Senn et al., 2018). The identity of the iron oxide formed after P depletion strongly depends on oxyanions in water. In oxyanion-free electrolytes such as our study formation of lepidocrocite is likely which could have caused the particle growth in the 30 min sample. Nevertheless, we conclude that more investigations are required to understand the P related observations from our study.

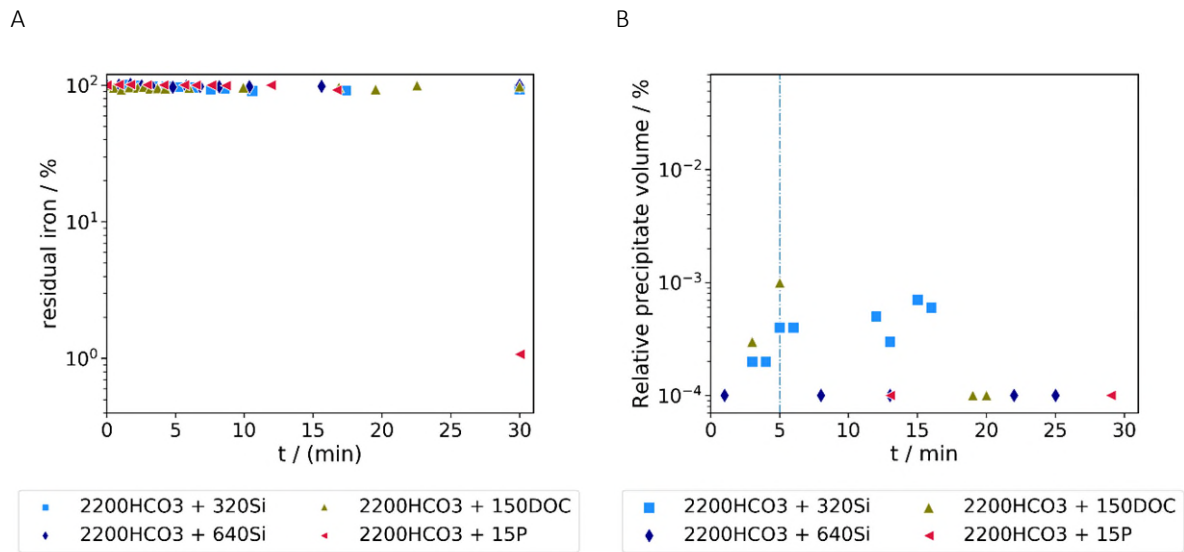


Figure 3: (A) Residual iron (%) after filtration through a 0.2µm filter and (B) precipitate volume relative to the total measured volume, as a function of different Si, P and NOM concentrations in the presence of 2200 µM HCO<sub>3</sub>.

### 3.3 Impact of calcium

The % of residual Fe after filtration through 0.20 µm filter and relative precipitate volume as a function of different HCO<sub>3</sub>, Si, P NOM concentrations in the presence of Ca are shown in Figure 4A and 4B respectively. The results in Figure 4A show that at constant Ca concentration of 900 µM, the efficiency of Fe removal decreases with increasing HCO<sub>3</sub> concentration. Without calcium, the removal was complete within 10 minutes for the HCO<sub>3</sub> additions (Figure 2A), but with the addition of 900 µM Ca the time to complete removal of Fe by 0.20 µM increases up to 30 minutes. These results needs further investigations to unravel the mechanisms responsible for this peculiar impact of Ca on Fe precipitation in the presence of HCO<sub>3</sub>.

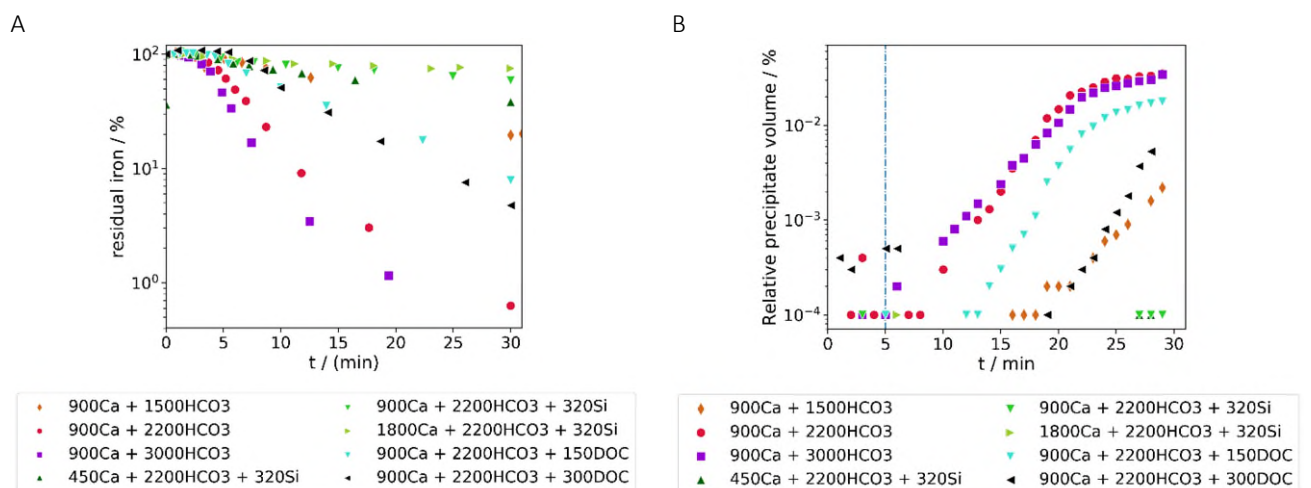


Figure 4: (A): residual iron (%) after passing through a 0.2µm filter and (B) precipitate volume relative to the total measured volume, both shown as time series. See Table 1: for explanation of the labels.



The addition of 450-1800  $\mu\text{M}$  Ca in  $\text{HCO}_3+\text{Si}$  solutions appears to slightly lower the residual Fe concentration (compare Figure 3A and Figure 4A), potentially attributed to charge neutralization and subsequent precipitate aggregation effect that the Ca ions create for the Si containing disordered Fe(III)(oxyhydr)oxides (Voegelin et al., 2010). Particles do hardly grow in size however, reaching to approximately 1 to 2  $\mu\text{m}$  after 30 minutes (Figure S1-C, supplementary material). The addition of Ca in the presence of 150-300  $\mu\text{M}$  DOC significantly improves the removal of Fe by 0.2  $\mu\text{m}$  filters, indicating effective growth and aggregation of the Fe(III), see Figure 4 and Figure S1-C (supplementary material) for the relative precipitate volume and  $d_{50}$  respectively. These results are in agreement with previous studies (Knocke et al., 1994; Sholkovitz and Copland, 1981). This can be explained based on the influence of DOC and Ca on the surface charge of the Fe precipitates. Because the NOM used in this study is largely composed of negatively charged humic substances, its complexation with Fe precipitates will increase the negative charge of the surface, thus hampering precipitate growth. However, when Ca is present in the solution, it can bind with these DOC-Fe complexes and reduce the surface charge to promote precipitate growth.

## 4 Conclusions and implications

We studied the precipitation of Fe in simulated groundwater solutions with different concentrations of  $\text{HCO}_3^-$ , Si, P, NOM and Ca, reflecting typical groundwater quality conditions in the Netherlands. We conclude that the different  $\text{HCO}_3^-$  concentrations have no significant impact on the precipitation of Fe and precipitation is completed in the typical residence time of groundwater treatment plants. Silicate additions in the presence of  $\text{HCO}_3^-$  result in reduced Fe precipitation, probably because of the negatively charged silicate-iron co-precipitate surfaces because this hampers precipitate growth. The additions of NOM in the presence of  $\text{HCO}_3^-$ , drastically hampers the precipitation growth of Fe, potentially due to the formation of soluble Fe(III)–NOM complexes. Phosphate and bicarbonate containing solutions initially hamper precipitate growth but more work is needed to conclude something definitive on the impact of P on Fe precipitation dynamics. Additions of Ca improves Fe precipitate growth in the presence of Si and NOM, potentially attributed to charge neutralization impact of Ca.

The implications of this study for groundwater treatment practice could be manifold. First, an expected increase in rain fall due to climate change, can cause the mobilization of NOM in drinking water sources, leading to increased levels of dissolved organic matter (DOM) and humic substances, alterations to their structure and reactivity (Lipczynska-Kochany, 2018). Lipczynska-Kochany also anticipates increased desorption from soil and sediments, as well as re-mobilization of metals and organic pollutants. In addition, the increased levels of acidic atmospheric  $\text{CO}_2$  participates increasingly in the weathering of carbonate and silicate minerals, leading to more bicarbonate,  $\text{Ca}^{+2}$  and other cations in drinking water sources (Qafoku, 2015). While a change in only bicarbonate does not alter (Fe) precipitation dynamics, changes calcium concentration does. This could be exploited by water utility operators for further optimisation of the iron removal efficiency. Moreover, precipitation dynamics are tightly linked with oxidation dynamics. As a result of the pre-aeration step in rapid sand filtration treatment, anaerobic groundwater containing Fe(II) oxidises via Fe(III) into Fe(hydr)oxides even in the absence of suspended particles or any other complexation agents by homogeneous chemical kinetics, also known as homogeneous oxidation (Davison & Seed, 1983; Moses & Herman, 1989). An auto-catalytic process, so-called heterogeneous oxidation, occurs if suspended precipitates allow for sorption and surface complexation with ferrous iron ions (Sharma, 2001; Werner Stumm & Sulzberger, 1992; Sung & Morgan, 1980). Heterogeneous oxidation is a dominant process in the removal of Fe by RSFs (Vries et al., 2016; Wolthoorn et al., 2004), but becomes retarded when P, Si or humic substances are present (Wolthoorn et al., 2004). Hence, (also) ionic strength and oxyanions can affect the rate of heterogeneous oxidation as well as the charge of Fe(III) (hydroxy)oxide precipitates, and leads to altered precipitation and coagulation characteristics.

Concluding, depending on aquifer characteristics and mineral weathering, the current operation of groundwater treatment sites might be in need of evaluation and further investigation whether additional measures are needed to keep Fe and other metal ion levels in drinking water at an acceptable level. For instance, in groundwater coming from calcareous soils, elevated levels of Ca and  $\text{HCO}_3^-$  enhances precipitation of Fe and coagulation of humic substances. Possible softening of the treated groundwater could therefore lead to a more effective overall treatment when placed after RSF and carry-over filtering and also allow reuse of calcite granules when calcite pellet contactors are used (Schetters et al., 2014; Tang et al., 2019). For optimisation of drinking water production and water source management under changing conditions, it is necessary to investigate the mechanisms that underpin the interplay of precipitation, colloidal stability and oxidation to arrive at an evidence based plant operation. This requires, amongst others, that the relation between precipitation rate and water composition as shown in this paper, needs to be quantified to eventually capture that in a model.



**Acknowledgements**

This research is financed by the Joint Research Programme of the Dutch Water Companies (BTO). Discussions with and feedback from the members of the project steering committee, i.e. Stephan van de Wetering, Simon Dost, Frank Schoonenberg, Ben Cools, and Alexander Rohling, have contributed to this work and are highly appreciated. We would like to thank prof. Emile Cornelissen (KWR, UGent) and the anonymous reviewers for their critical review of the paper.

# I References

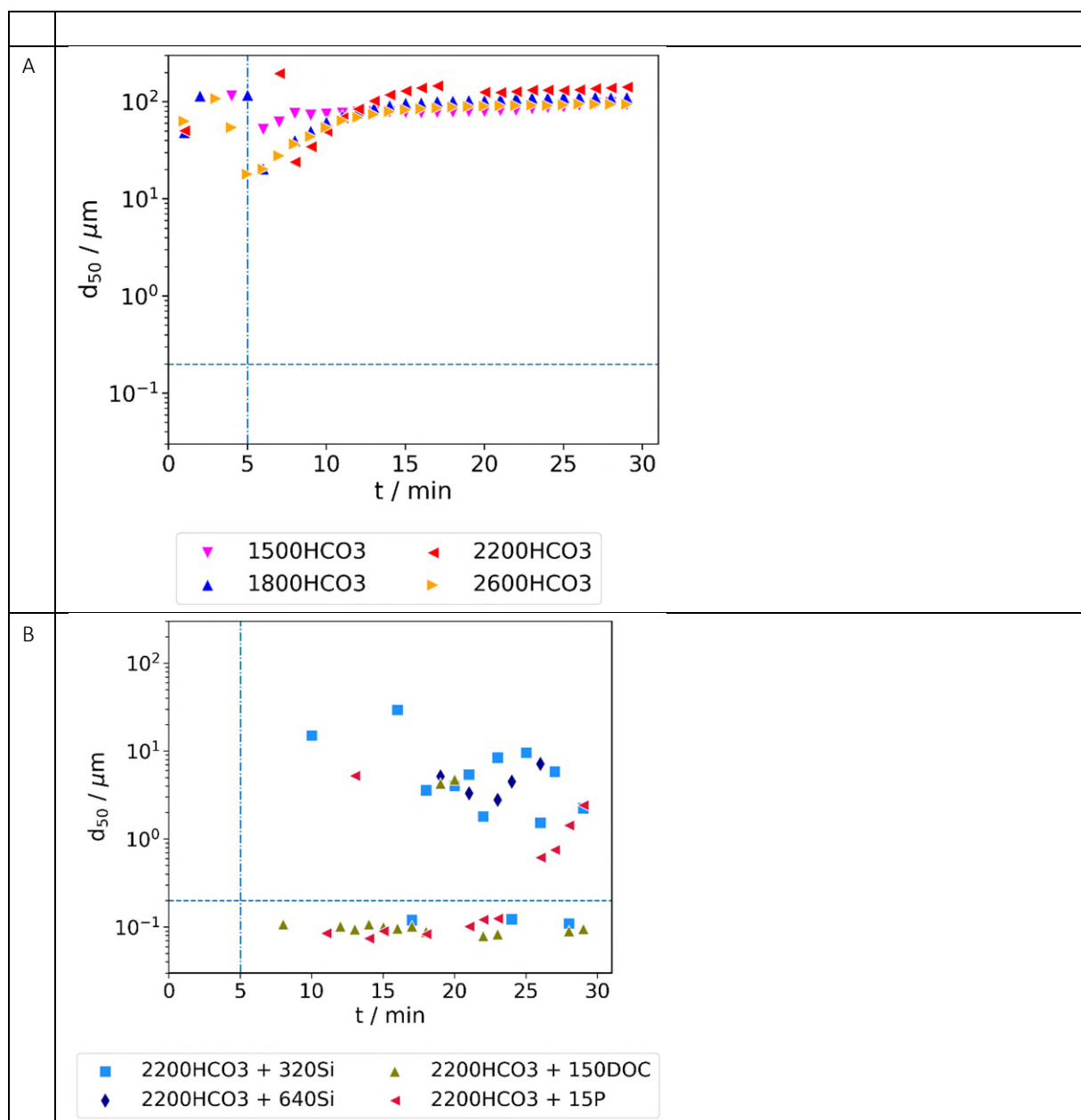
- Ahmad, A., Rutten, S., Eikelboom, M., de Waal, L., Bruning, H., Bhattacharya, P., van der Wal, A., 2020. Impact of phosphate, silicate and natural organic matter on the size of Fe(III) precipitates and arsenate co-precipitation efficiency in calcium containing water. *Sep. Purif. Technol.* 235, 116117. <https://doi.org/10/ggf86k>
- Bratby, J., 2016. *Coagulation and Flocculation in Water and Wastewater Treatment*. IWA Publishing.
- Harif, T., Khai, M., Adin, A., 2012. Electrocoagulation versus chemical coagulation: Coagulation/flocculation mechanisms and resulting floc characteristics. *Water Res.* 46, 3177–3188. <https://doi.org/10/ghpnj9>
- Jarvis, P., Jefferson, B., Parsons, S.A., 2006. Floc structural characteristics using conventional coagulation for a high doc, low alkalinity surface water source. *Water Res.* 40, 2727–2737. <https://doi.org/10/c33jnp>
- Jobin, R., Ghosh, M.M., 1972. Effect of buffer intensity and organic matter on the oxygenation of ferrous iron. *J. Am. Water Works Assoc.* 64, 590–595.
- Knocke, W.R., Shorney, H.L., Bellamy, J.D., 1994. Examining the reactions between soluble iron, DOC, and alternative oxidants during conventional treatment. *J. - Am. Water Works Assoc.* 86, 117–127. <https://doi.org/10/gftfhv>
- Lipczynska-Kochany, E., 2018. Effect of climate change on humic substances and associated impacts on the quality of surface water and groundwater: A review. *Sci. Total Environ.* 640–641, 1548–1565. <https://doi.org/10/gjnz2x>
- Lips, A., Willis, E., 1973. Low angle light scattering technique for the study of coagulation. *J. Chem. Soc. Faraday Trans. 1 Phys. Chem. Condens. Phases* 69, 1226–1236. <https://doi.org/10/cxp4vn>
- Mastersizer 2000 user manual, n.d.
- Qafoku, N.P., 2015. Chapter Two - Climate-Change Effects on Soils: Accelerated Weathering, Soil Carbon, and Elemental Cycling, in: Sparks, D.L. (Ed.), *Advances in Agronomy*. Academic Press, pp. 111–172. <https://doi.org/10.1016/bs.agron.2014.12.002>
- Santana-Casiano, J.M., González-Dávila, M., Millero, F.J., 2004. The oxidation of Fe(II) in NaCl–HCO<sub>3</sub><sup>-</sup> and seawater solutions in the presence of phthalate and salicylate ions: a kinetic model. *Mar. Chem.* 85, 27–40. <https://doi.org/10/fbnh3v>
- Schettters, M.J.A., van der Hoek, J.P., Kramer, O.J.I., Kors, L.J., Palmén, L.J., Hofs, B., Koppers, H., 2014. Circular economy in drinking water treatment: reuse of ground pellets as seeding material in the pellet softening process. *Water Sci. Technol.* 71, 479–486. <https://doi.org/10/f64858>
- Sholkovitz, E.R., Copland, D., 1981. The coagulation, solubility and adsorption properties of Fe, Mn, Cu, Ni, Cd, Co and humic acids in a river water. *Geochim. Cosmochim. Acta* 45, 181–189. <https://doi.org/10/fbs5qw>
- Tang, C., Jørgensen Hedegaard, M., Lopato, L., Albrechtsen, H.-J., 2019. Softening of drinking water by the pellet reactor - Effects of influent water composition on calcium carbonate pellet characteristics. *Sci. Total Environ.* 652, 538–548. <https://doi.org/10/gjn2q5>
- Tipping, E., 1993. Modeling the competition between alkaline earth cations and trace metal species for binding by humic substances. *Environ. Sci. Technol.* 27, 520–529. <https://doi.org/10/fcdjb7>
- van den Hoop, M.A.G.T., van Leeuwen, H.P., Pinheiro, J., Mota, A.M., Simões Gonçalves, M. de L., 1995. Voltammetric analysis of the competition between calcium and heavy metals for complexation by humic material. *Colloids Surf. Physicochem. Eng. Asp.* 95, 305–313. <https://doi.org/10/fbzxtj>
- Vries, D., Bertelkamp, C., Schoonenberg-Kegel, F., Hofs, B., Dusseldorp, J., Bruins, J., de Vet, W., van den Akker, B., 2016. Iron and manganese removal: Recent advances in modelling treatment efficiency by rapid sand filtration. *Water Res.* 35–45. <https://doi.org/10/gftf3g>

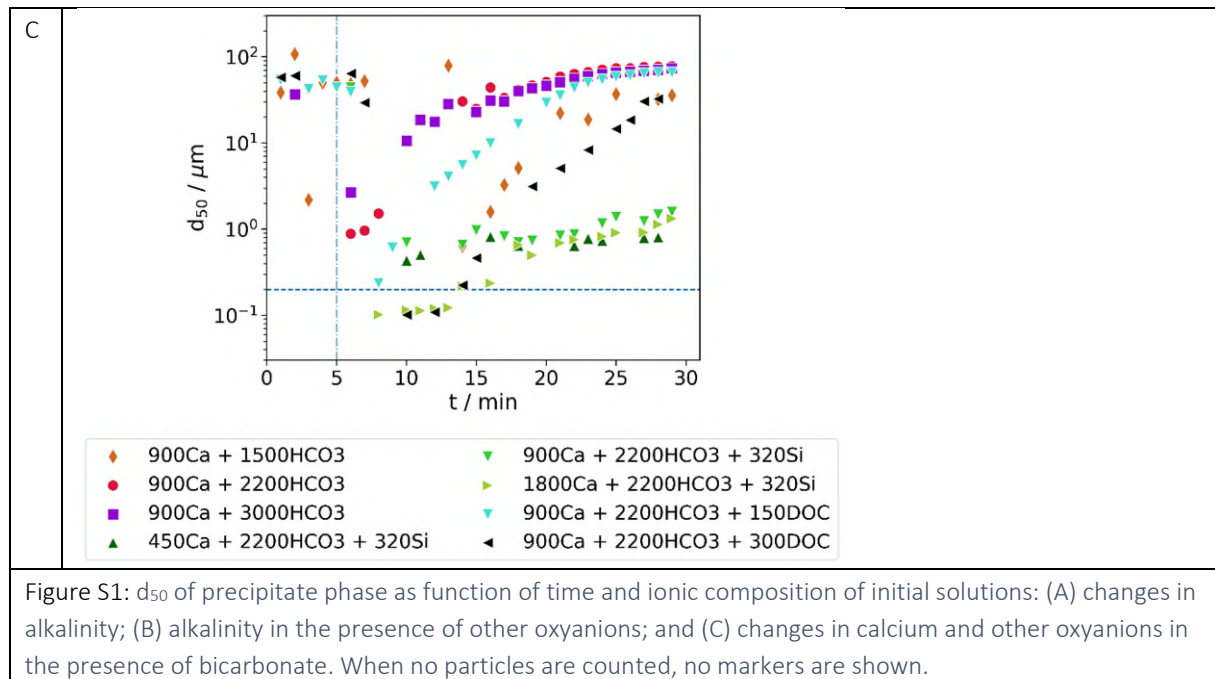
Wolthoorn, A., Temminghoff, E.J., Weng, L., van Riemsdijk, W.H., 2004. Colloid formation in groundwater: effect of phosphate, manganese, silicate and dissolved organic matter on the dynamic heterogeneous oxidation of ferrous iron. *Appl. Geochem.* 19, 611–622.  
<https://doi.org/10/fpn7mm>

## II Supplementary material

### II.I Particle size

The particle size distribution of the precipitates is derived from the relative precipitate volume using Mie theory in order to develop a scattering pattern that matches the measured pattern (Harif et al., 2012; Lips and Willis, 1973). From the size distribution measurements, only the  $d_{50}$  is presented in Figure S1, i.e. the size where 50% of the particles have a smaller or equal diameter. Note that results with an obscuration lower than 2 to 3% is considered as unreliable, hence no conclusive remarks can be made regarding precipitation kinetics during the intense stirring phase that ends at  $t = 5$  minutes ("Mastersizer 2000 user manual," n.d.).







## II.II NOM solution characteristics

Table S1. NOM characterization of a solution of ultrapure water spiked with NF concentrate to achieve ca. 3 mg/L DOC, obtained by LC-OCD analysis

DOC - Dissolved	$\mu\text{g/l C}$	3140
DOC - HOC, hydrophobic	$\mu\text{g/l C}$	451
DOC - CDOC, hydrophilic	$\mu\text{g/l C}$	2689
CDOC - Bio-polymers	$\mu\text{g/l C}$	6
CDOC - Bio-polymers - DON	$\mu\text{g/l N}$	3
CDOC - Bio-polymers - N/C	$\mu\text{g}/\mu\text{g}$	0.51
CDOC - Bio-polymers - Proteins	%	unknown
CDOC - Humic substances (HS)	$\mu\text{g/l C}$	2370
CDOC - Humic substances - DON	$\mu\text{g/l N}$	30
CDOC - Humic substances - N/C	$\mu\text{g}/\mu\text{g}$	0,01
CDOC - Humic substances - Aromaticity	$\text{L}/(\text{mg}*\text{m})$	3,82
CDOC - Humic substances - Mol-Weight	$\text{g}/\text{mol}$	749
CDOC - Building Blocks	$\mu\text{g/l C}$	183
CDOC - LMW acids	$\mu\text{g/l C}$	<1
CDOC - LMW Neutrals	$\mu\text{g/l C}$	130
Inorganic Colloidal (SAC)	$\text{m}^{-1}$	<0.01
SUVA (SAC/DOC)	$\text{L}/(\text{mg}*\text{m})$	3.18

## II.III Iron removal efficiency

At  $t=30$  minutes, i.e. 30 minutes after aeration has started, samples have been collected by  $0.20 \mu\text{m}$  syringes and measured with ICP-MS to determine Fe removal. Removal efficiencies have been calculated for total iron (i.e. the sum of ferrous and ferric iron) and is shown in Figure S1.

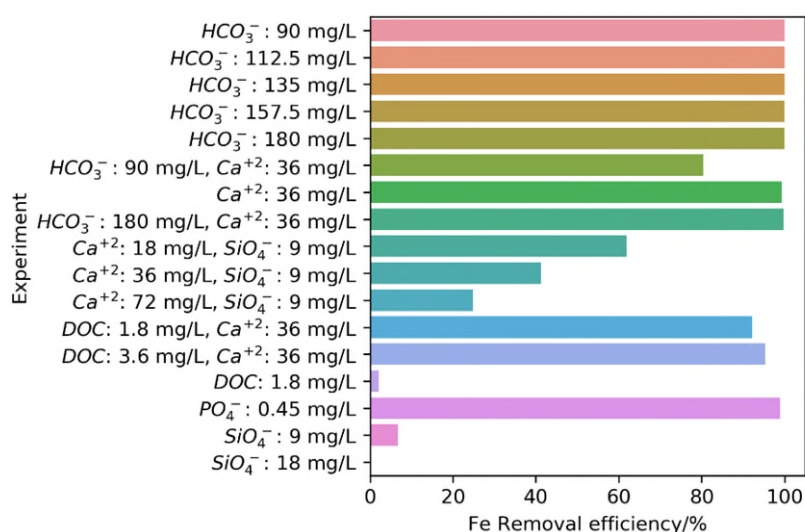


Figure S2: removal efficiency of total iron after 30 minutes of aeration. Removal efficiency of  $\text{SiO}_4^-$  is zero.

## II.IV Dissolved oxygen

In Figure S3, the dissolved oxygen is shown as percentage of an oxygen saturated solution are shown for all experiments. For all, but two experiments, the DO attain values of 85% or higher.

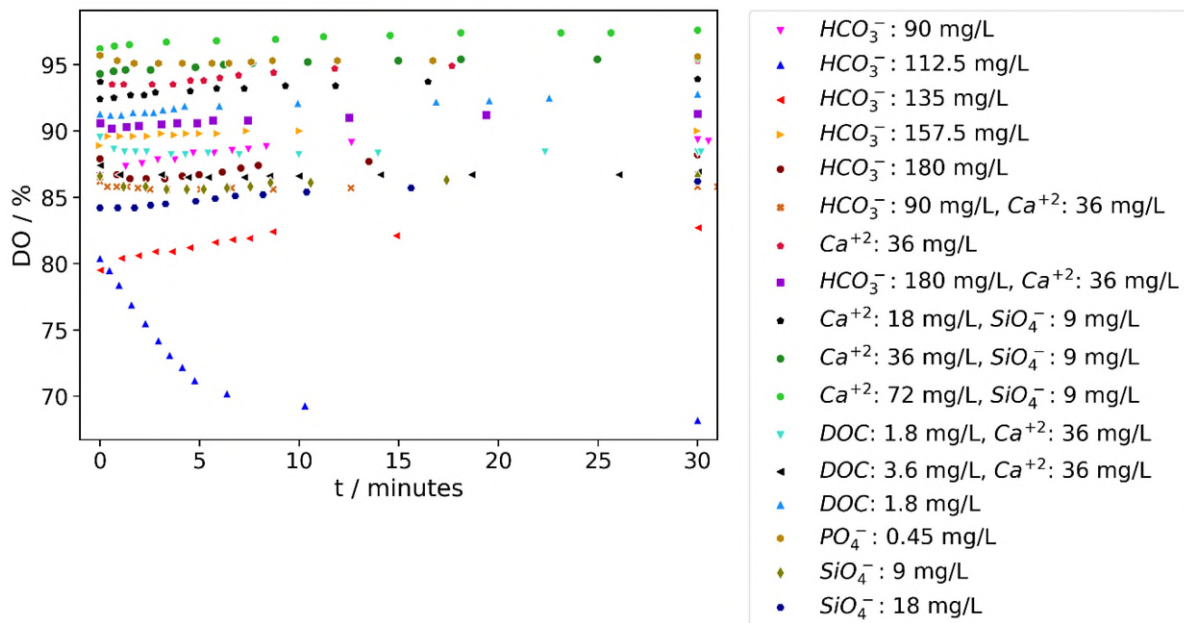


Figure S3 – dissolved oxygen concentration (DO) as percentage of an oxygen saturated solution. Shown for different experiments

## II.V Apparent iron oxidation rate constants

In Figure S4, the apparent iron oxidation rate constant according to (Santana-Casiano et al., 2004) are shown. The water composition of Table 1 are used in combination with the same thermodynamic constant and the kinetic rate constants of all iron species as used by (Santana-Casiano et al., 2004).

The apparent rate constant  $k_{app}$  is defined as:

$$\frac{d\{Fe(II)\}}{dt} = -k_{app}[O_2]\{Fe(II)\}$$

where  $\{Fe(II)\}$  is the total Fe(II) concentration in the solution and  $[O_2]$  the oxygen concentration in the solution.

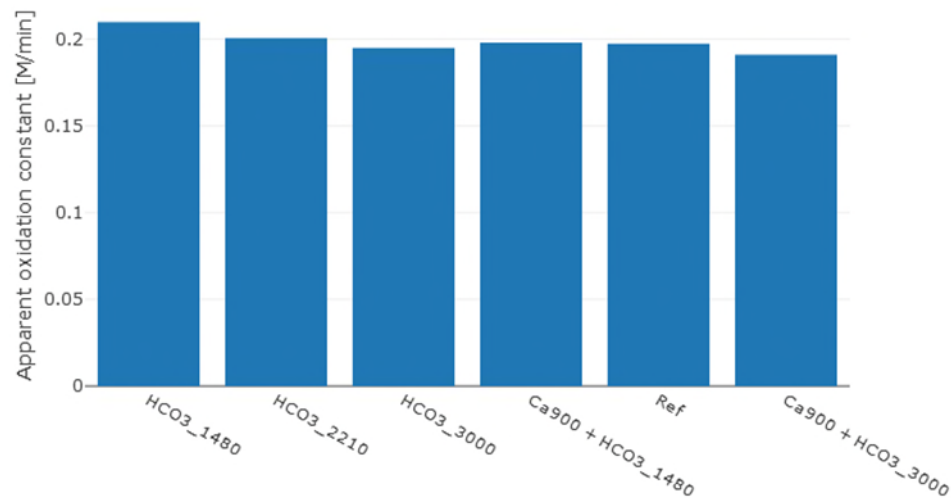


Figure S4 apparent homogeneous iron oxidation rate constants according to (Santana-Casiano et al., 2004) for different bicarbonate and calcium containing waters.

## References

Santana-Casiano, J.M., González-Dávila, M., Millero, F.J., 2004. The oxidation of Fe(II) in NaCl–HCO<sub>3</sub><sup>–</sup> and seawater solutions in the presence of phthalate and salicylate ions: a kinetic model. *Mar. Chem.* 85, 27–40. <https://doi.org/10/fbnh3v>